

E-ISSN: 2709-9423

P-ISSN: 2709-9415

JRC 2022; 3(2): 23-29

© 2022 JRC

[www.chemistryjournal.net](http://www.chemistryjournal.net)

Received: 19-04-2022

Accepted: 24-05-2022

**Karthick Muniraj**School of Bioscience and  
Biotechnology VIT University  
Vellore, Tamil Nadu, India**Priyanka Saha**School of Bioscience and  
Biotechnology VIT University  
Vellore, Tamil Nadu, India**Tripathy M**Assistant Professor,  
Department of zoology  
University of Delhi, Delhi,  
India

## Synthesis of silver doped TiO<sub>2</sub> nanoparticles (Ag-TiO<sub>2</sub>) photocatalytic degradation of methyl red under sunlight

**Karthick Muniraj, Priyanka Saha and Tripathy M**

### Abstract

Silver-doped TiO<sub>2</sub> nanoparticles (Ag-TiO<sub>2</sub>) were successfully synthesized by the synthesized hydrolysis method. photocatalyst as efficiently used for degradation of methyrad dye under direct sunlight 23 radiation. towtypes mol (3mol% and 6mol%) doped Ag-TiO<sub>2</sub> nanoparticles Subsequent characterization of synthesized photocatalysts was characterization using PXRD, EDX, FT-IR, Photoluminescence and. UV-Vis The degradation studies revealed that initial rate of photocatalytic degradation of methyrad using Ag-TiO<sub>2</sub> nanopaticles. Introduction Heterogeneous semiconductor photocatalysis using titanium dioxide (TiO<sub>2</sub>) has been extensively explored for oxidative degradation of various organic and inorganic pollutants in air/water environment due to its strong oxidation power, high photocatalytic degradation ability, chemical and biological stability, longterm stability against photo- and chemical corrosion, low cost, abundance and environmental-friendliness.

**Keywords:** TiO<sub>2</sub> methyrad, sunlight

### Introduction

The broad usage of synthetic dyes in variety of industrial sectors have led to the pollution of aquatic ecosystem by effluent discharge from the dyeing industries. In many circumstances these colours prevent the sunlight penetration in Water thus affecting the photosynthesis of the aquatic species (*et al*). In photocatalytic degradation process the catalyst is induced by the UV light present in sunrays. Thus the activated nanoparticle orchestrates a redox process that degrades the chemical dyes. Among many materials Titanium Oxide TiO<sub>2</sub>, transition metal oxide is widely used for the photocatalytic degradation but in this study silver is doped as it has low toxicity and helps in the rapid degradation of methyl red. TiO<sub>2</sub> Being in the near UV to visible light region can use the sun light and help in the active degradation of dyes. These TiO<sub>2</sub> particles can be later separated from the effluent and can be used again.

### Experiment

#### Reagents and chemicals

Titanium isopropoxide, (titanium tetraisopropoxide or titanium IV isopropoxide) (TTIP), silver nitrate (99.9% pure), Ethanol (99%), Deionized water, distilled water, isopropyl alcohol were purchased from sigma Aldrich.

#### Preparation of TiO<sub>2</sub> nanoparticales

Titanium di oxide (TiO<sub>2</sub>) nanoparticles were prepared by Hydrolysis method. Titanium (IV) isoprop oxide (Ti[OCH(CH<sub>3</sub>)<sub>2</sub>]<sub>4</sub>) as dissolved in 100 ml of isopropyl alcohol ((CH<sub>3</sub>)<sub>2</sub>CHOH) and solution was stirred continuously for 1 h in room temperature cool in 20min After adding 500 ml of deionized water was added suddenly to the above prepared mixture. The resultant solution was aged for 2 h, then centrifuged, (Zhou, Rui, *et al.*) washed several times with deionized water and ethanol and dried at 100°C in hot plate. The preparation of the TiO<sub>2</sub> nanoparticles was then completed by calcinating prepared materials at 450°C for 60 min in furnace.

#### Syntheses of Silver Nanopartical Ag NPs

Take 50 mL deionised water added to 0.5 g of tangerine peel. The mixture was boiled at room temperature for 40 min. using in filter paper was filtered solution then added to silver nitrate solution (10-5 M) at 25 Co with stirring.

**Correspondence****Karthick Muniraj**School of Bioscience and  
Biotechnology VIT University  
Vellore, Tamil Nadu, India

Change the color due the reduction of silver ions into silver nanoparticles and the formation of silver nanoparticles can be visually observed (Alahrani, E. *et al.* 2015).

### Ag-doped TiO<sub>2</sub> synthesis

Ag-doped TiO<sub>2</sub> was synthesized using 0.5 g of TiO<sub>2</sub> was added to 100 mL of AgNO<sub>3</sub> aqueous solution containing 1. g of Ag<sub>2</sub>O per 100 g TiO<sub>2</sub> under vigorous stirring (600 rpm for 60 min at room temperature). The pH of the suspension was adjusted to 7 using 0.1 M NH<sub>4</sub>OH to achieve better adsorption of Ag<sub>2</sub>O onto TiO<sub>2</sub> support After reaching Ag<sub>2</sub>O sorption equilibration, the solution was centrifuged at 3500 rpm for 15min to separate Ag<sub>2</sub>O/TiO<sub>2</sub> from water. (Rao CV *et al.* 2016). Ag<sub>2</sub>O/TiO<sub>2</sub> residue was then dispersed in 25 mM L-ascorbic acid aqueous solution and stirred for 25 min. Upon the addition of ascorbic acid, a change in the color of the suspension from milky white to brown was observed which indicates the reduction of Ag<sub>2</sub>O to Ag<sup>0</sup>. The residue was then filtered out using a 0.2 mm membrane filter and washed four times with ethanol-water mixture and with DI water to remove loosely bound and/or undoped Ag<sub>2</sub>O on TiO<sub>2</sub>. Finally, the residue was dried. In rutile structure of TiO<sub>2</sub>, different 3mol% Ag-TiO<sub>2</sub>. and 6mol% Ag-TiO<sub>2</sub>, each oxygen atoms were enclosed by three tin atoms and each tin atoms were surrounded by six oxygen atoms The calculated crystallite size of the TiO<sub>2</sub> and Ag-TiO<sub>2</sub> was found to be TiO<sub>2</sub> for (8.128 nm), 3mol% Ag-TiO<sub>2</sub> (7.460 nm) and 6mol% Ag-TiO<sub>2</sub> (9.566 nm) in a hot air oven at 100 C for 10 h. The synthesized photocatalyst codes along with their

nominal and true load synthesis different method (Devipriya Gogoi. *et al.* 2019)

## Results and Discussion

### X-Ray diffraction Analysis

X-Ray Diffraction pattern of synthesized Titanium Dioxide nanoparticles. For The diffraction peaks of TiO<sub>2</sub> and two mol variation of doping we add 3mol% Ag-TiO<sub>2</sub> and 6mol% Ag-TiO<sub>2</sub>, the peaks observed for TiO<sub>2</sub> at 25.39°, 48.14°, 37.97°, 55.08°, 62.77°, 68.92°, 70.38°, 75.10° corresponds to as (101) (411) (200) (105) (211) (116) (220) and (215) planes of anatase phase of TiO<sub>2</sub>. planes, respectively. Then for Ag doped TiO<sub>2</sub>, all the diffraction peaks can be perfectly indexed to the tetragonal anatase phase and crystallographic space group which is well matched with standard and 0.598 Ag-TiO<sub>2</sub> (a = b = 2.5967Å, c = 8.3590 Å). The preferred peak for 2θ at 25.35° was observed with corresponding plane. Which is the strongest peak for all the TiO<sub>2</sub> nanoparticles calcined at 450 °C, confirms the Anatase TiO<sub>2</sub> and polycrystalline nature of TiO<sub>2</sub>. In rutile structure of TiO<sub>2</sub>, different 3mol% Ag-TiO<sub>2</sub> and 6mol% Ag-TiO<sub>2</sub>, each oxygen atoms were enclosed by three tin atoms and each tin atoms were surrounded by six oxygen atoms which were situated at corners of equilateral triangle and regular octahedron respectively. The average crystallite size of the synthesized nanoparticle. The calculated crystallite size of the TiO<sub>2</sub> and Ag- TiO<sub>2</sub> was found to be TiO<sub>2</sub> for (8.128nm), 3mol% Ag-TiO<sub>2</sub> (7.460nm) and 6mol% Ag-TiO<sub>2</sub> (9.566nm).

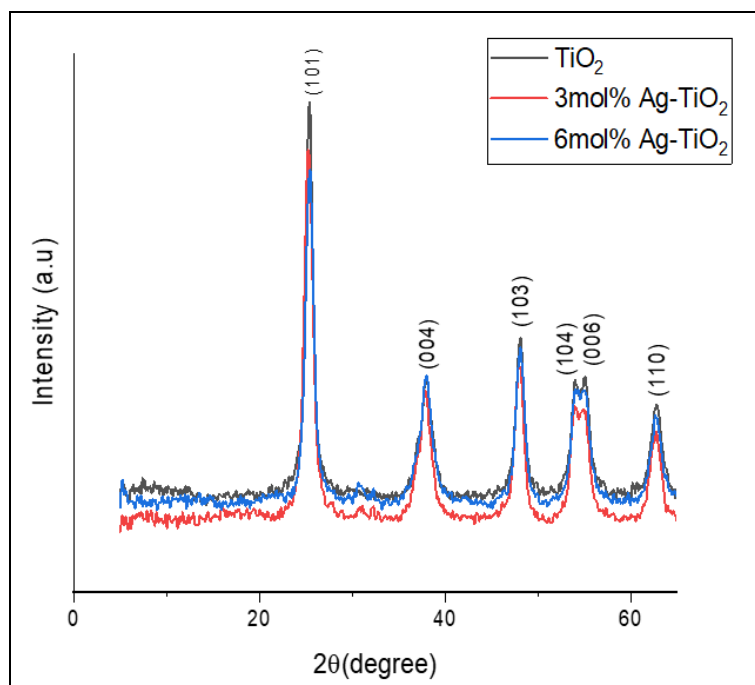


Fig 1: X-Ray Diffraction pattern of TiO<sub>2</sub>, 3mol% Ag-TiO<sub>2</sub> and 6mol % Ag-TiO<sub>2</sub>

Table 1: Lattice parameters of synthesized materials

Name of the sample	Lattice parameters (Å)		c/a ratio
	a = b	c	
TiO <sub>2</sub>	3.7714	8.7217	2.3125
3mol% Ag- TiO <sub>2</sub>	2.5967	8.3590	3.2190
6mol% Ag- TiO <sub>2</sub>	2.3882	9.7324	4.0752

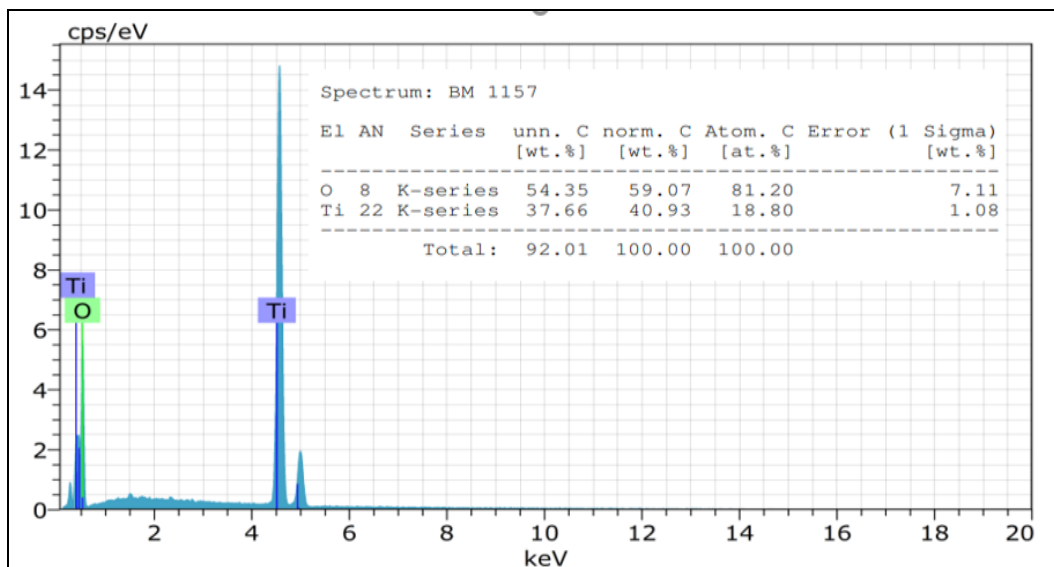
**Table 2:** Various structure parameters estimated from XRD pattern.

Sample name	Crystallite size D (nm)	Dislocation density ( $\delta$ ) ( $\times 10^{15}$ lines/m <sup>2</sup> )	Micro strain ( $\epsilon$ ) ( $\times 10^{-3}$ /lines <sup>2</sup> m <sup>4</sup> )	Unit cell volume ( $\text{\AA}^3$ )
TiO <sub>2</sub>	8.128	165.8155	13.3120	124.0497
3mol% Ag- TiO <sub>2</sub>	7.460	203.4990	15.8886	56.3667
6mol% Ag- TiO <sub>2</sub>	9.566	187.9120	14.8044	55.5120

**Energy dispersive X-ray analysis (EDX):**

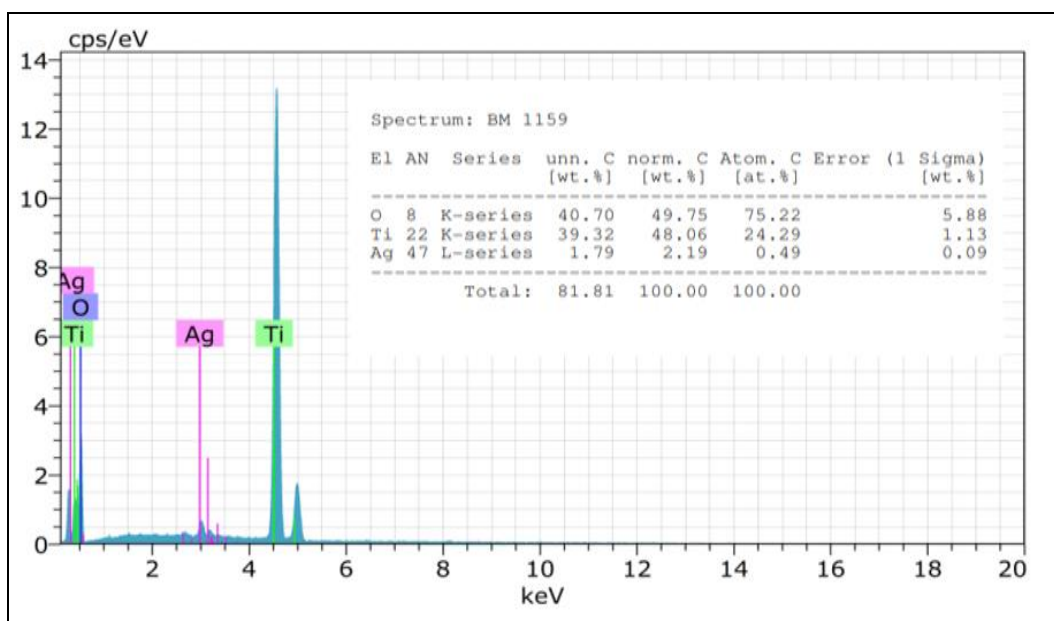
The energy dispersive X-ray analysis (EDX) spectrum was shown in Figure 1. The EDAX spectrum indicates the

presence of Ti and O which confirms the formation of TiO<sub>2</sub> in the sample. The presence of other elements is also due to the adoption of hydrolysis method.

**Fig 2:** EDX spectrum of TiO<sub>2</sub> nanoparticles

The EDAX spectrum shown in Figure 2. Indicates the presence of Ag, Ti and O which confirms the formation of

TiO<sub>2</sub> in the sample. The presence of elements is also due to the adoption of hydrolysis method.

**Fig 3:** EDX Spectrum of Ag-TiO<sub>2</sub> Nanoparticles**UV-Visible spectroscopic analysis:**

Optical measurements were performed by using Uv-Vis spectra, Figure 3 shows the absorbance spectra of synthesized TiO<sub>2</sub> nanoparticles, recorded with the spectrum in the range of 200 - 1000 nm. The optical absorption spectra are expected to influence on various features such as oxygen deficiency, surface roughness and impurity centres.

The absorbance peak was observed at 345 nm for synthesized TiO<sub>2</sub> nanoparticles which may be due to electronic transition from the valance band to conduction band. The absorption spectra revealed that the absorption edge of TiO<sub>2</sub> were blue shifted. Fewer molecular orbitals are added to the possible energy state of the molecule. Hence absorbance occurs at high energies, so shift occurs towards

shorter wavelength. Also, the direct transition is more favourable in anatase  $\text{TiO}_2$  nanoparticles. Absorbance energy shifted to higher energy. Blue shift occurs when crystalline size decreases obtained from Tauc's plot by using UV-Vis spectra, Figure 4, Figure 5 and Figure 6 shows the absorbance spectra of synthesized 3 mol% Ag- $\text{TiO}_2$  nanoparticles, recorded with the spectrum in the range of

200 - 1000 nm. The absorbance peak was observed at 342 nm for synthesized Ag- $\text{TiO}_2$  nanoparticles which may be due to electronic transition from the valance band to conduction band. And 6 mol% Ag- $\text{TiO}_2$  nanoparticles, recorded with 200-900 nm. The absorbance peak was observed at 346 nm. UV absorbance spectra and Optical band gap of 6 mol% Ag- $\text{TiO}_2$  nanoparticles.

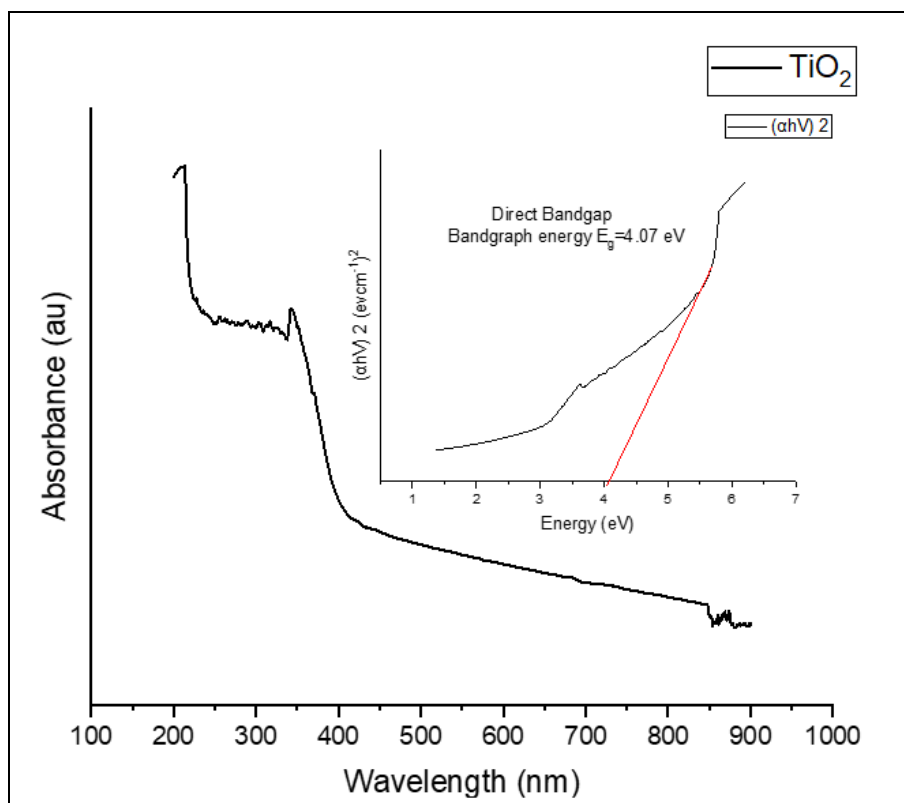


Fig 4: UV absorbance spectra and Optical band gap of  $\text{TiO}_2$  nanoparticles

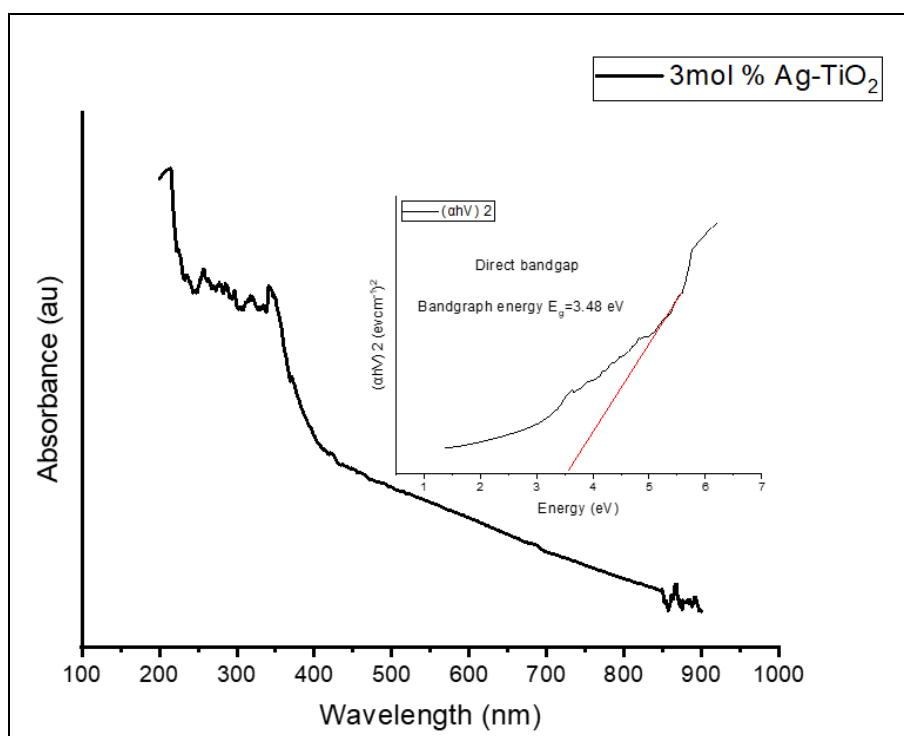
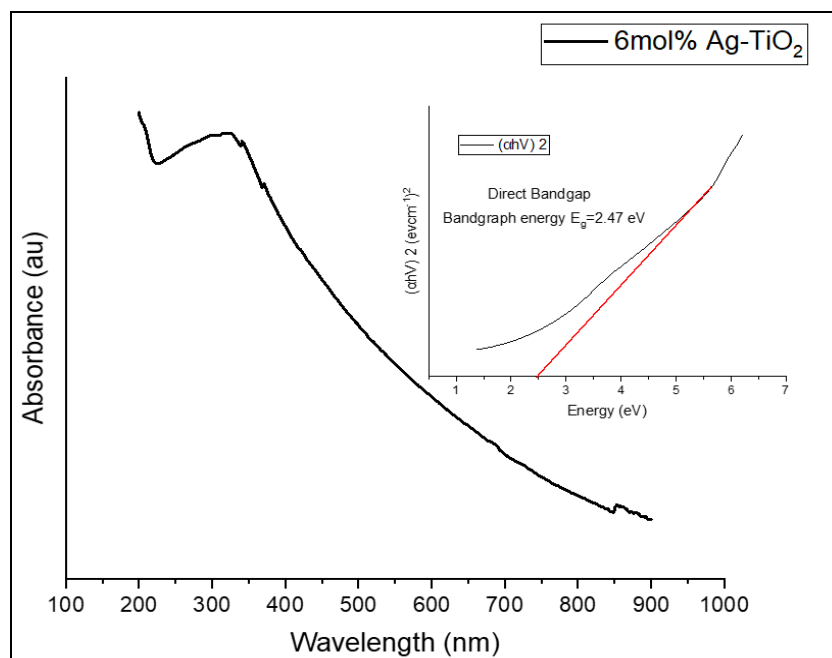


Fig 5: UV absorbance and optical band gap of 3mol% Ag- $\text{TiO}_2$  Nanoparticles



**Fig 6:** UV absorbance and optical band gap of 6mol% Ag- TiO<sub>2</sub> Nanoparticles

**Table 3:** Energy Band gap of sample

Sample	Band gap energy
TiO <sub>2</sub>	4.07
3 mol% Ag-TiO <sub>2</sub>	3.48
6 mol% Ag-TiO <sub>2</sub>	2.47

#### Photoluminescence spectroscopic analysis

The photoluminescence spectroscopic technique has been widely used to investigate structures and defects of metal oxide semiconductors. The photoluminescence spectra of synthesised TiO<sub>2</sub> nanoparticles such as 3 mol% Ag-TiO<sub>2</sub> and 6 mol% Ag-TiO<sub>2</sub> recorded with excitation wavelength of 320 nm were shown in Figure 7. The PL emission peaks were observed at 321 nm, 400 nm, 425 nm, 489 nm and 534

nm. The small peak represents the emission linked to defects such as oxygen vacancies respectively. The peaks appeared in PL spectra of the doped TiO<sub>2</sub> are almost observed at the same locations of those found in pure TiO<sub>2</sub>. This refers to the inhibition occurring in photo-generated electron recombination from the conduction band to valence band of TiO<sub>2</sub>. From the graphs obtained for Ag-TiO<sub>2</sub> nanoparticles it can be noticed that of 3 mol% and 6 mol% Ag into the TiO<sub>2</sub> matrix quenches the fluorescence intensity by a significant level. It can be noticed that the maximum increment in the absorption. The reduced intensity of PL spectra implies the suppression of the recombination rate of electron-hole pairs which favours the photocatalytic degradation efficiency.

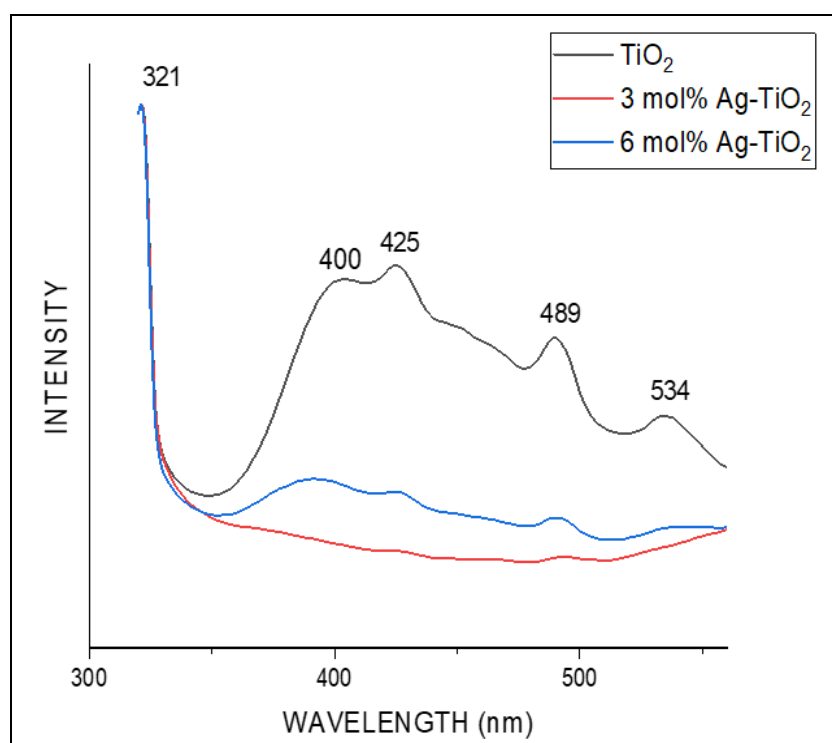


**Fig 7:** PL SPECTRA OF TiO<sub>2</sub>, 3 mol% Ag - TiO<sub>2</sub> and 6 mol% Ag - TiO<sub>2</sub>

### Photocatalytic activity

In order to validate the prepared  $\text{TiO}_2$ , 3 mol%  $\text{Ag-TiO}_2$  and 6 mol%  $\text{Ag-TiO}_2$  Illumination without  $\text{TiO}_2$ , 3 mol%  $\text{Ag-TiO}_2$  and 6 mol%  $\text{Ag-TiO}_2$  NPs also does not result in the degradation of dyes. Therefore, the presence of both light illumination and  $\text{TiO}_2$ , 3 mol%  $\text{Ag-TiO}_2$  and 6 mol%  $\text{Ag-TiO}_2$  NPs are necessary for the efficient degradation of dyes (8). It is observed from Fig 8 that the degradation rate of Methyl red (MR) increases with UV irradiation time and the photocatalytic activity is improved when  $\text{TiO}_2$  is doped with Ag atoms. Pure  $\text{TiO}_2$  shows degradation of MR after  $\approx 1$  h of UV exposure whereas,  $\text{Ag-TiO}_2$  sample shows degradation after 30 min, it is the highest degradation

efficiency recorded (2-8). When radiations of certain energy (UV or Visible) fall on  $\text{TiO}_2$  and  $\text{Ag-TiO}_2$  photocatalyst surface with energy (hm) equal to or higher than bandgap of catalyst, electrons ( $e^-$ ) initially at valence band (VB) gains energy and transfer to conduction band (CB) by leaving holes ( $h^+$ ) at VB. Now, the generated holes ( $h^+$ ) react with  $\text{H}_2\text{O}$  to form OH radicals. Similarly, photogenerated  $e^-$  migrates to surface of catalyst, which act as an  $e^-$ -acceptor, results in generation of superoxide anion radicals ( $\text{O}_2^-$ ). Both  $\text{O}_2^-$  and OH radicals are responsible for degradation of organic pollutants like dyes. The possible reaction mechanism can be proposed as follows and the schematic are shown in Fig. 9 and Fig 10.

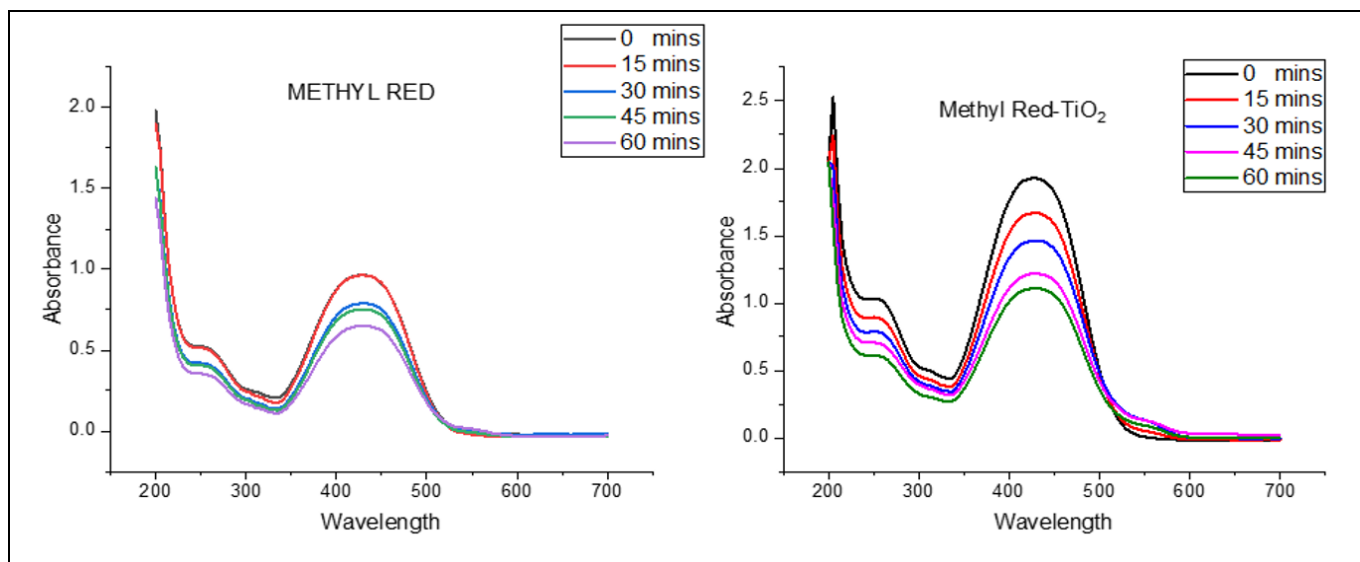


Fig 8: Photocatalytic degradation of MRdyes under sunlight illuminations

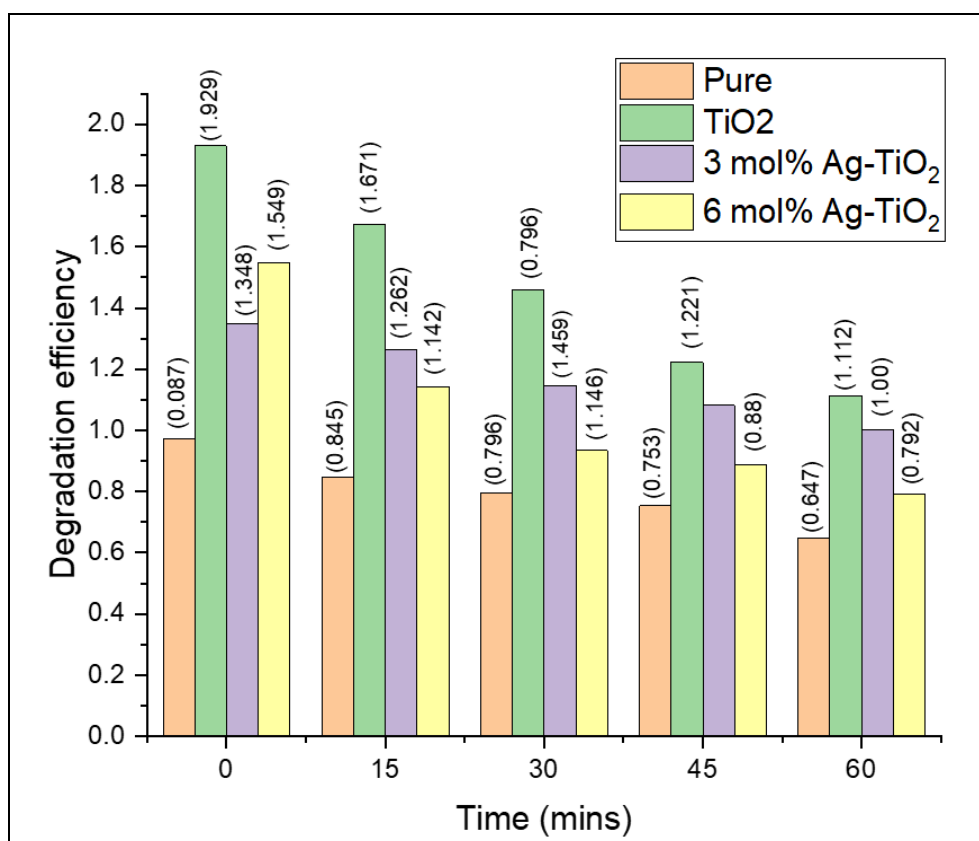


Fig 9: Graphs Indicating Photocatalytic degradation of combine sample

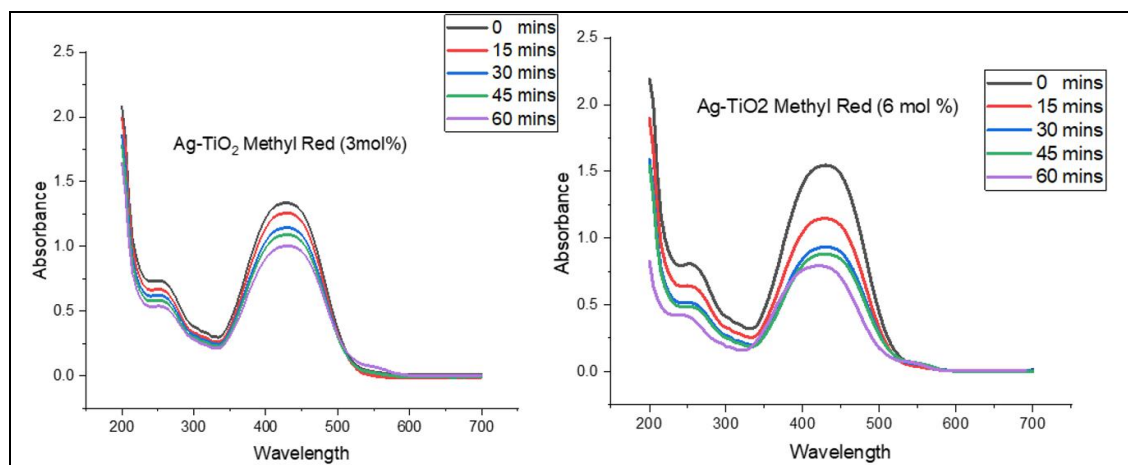


Fig 10: Photocatalytic degradation of Ag-TiO<sub>2</sub> under sunlight illuminations

### Conclusion

The aim of the present work, the nanoparticles of pure and Ag doped TiO<sub>2</sub> were prepared by hydrolysis method. TiO<sub>2</sub> nanoparticles and Ag doped TiO<sub>2</sub> formed were characterized structurally (XRD), Optically UV and PL, EDX. From the obtained results, we have drawn out the following conclusions besides proposing some aspects for potential future works. The powder X-ray diffraction studies reveal the polycrystalline nature of prepared TiO<sub>2</sub> and Ag-TiO<sub>2</sub> nanoparticles very well matches with. The average crystalline size of the TiO<sub>2</sub> for (8.128nm), 3mol% Ag-TiO<sub>2</sub> (7.460nm) and 6mol% Ag-TiO<sub>2</sub> (9.566 nm) by employing Debye - Scherrer's formula. It possesses Tetragonal structure with crystallographic space group of P42/mnm, and various structural parameters like dislocation density, micro strain, lattice parameter, was determined (1). The UV absorbance spectra reveals the absorbance edge of the synthesized nanoparticles were blue shifted. The optical band gap energy of the prepared material was TiO<sub>2</sub>, 3 mol% Ag-TiO<sub>2</sub> and 6 mol% Ag-TiO<sub>2</sub> (4.07eV, 3.48eV and 2.16eV) obtained from Tauc's plot. The photoluminescence spectra show the emission peaks of the synthesized materials observed at 321 nm, 400 nm, 425 nm, 489 nm and 534 nm. The peak at 340 nm maybe due to emission of bandgap transition and excitonic photoluminescence spectra resulting from the surface oxygen vacancy and defects The EDX analysis confirms the presence of respective elements in the prepared nanoparticles, and it confirms that no other elements involved in the nanoparticles (3). Nanoparticles which are used in photocatalytic degradation. The Ag nanoparticles are found to enhance the TiO<sub>2</sub> photocatalytic activity. The MR photo degradation was carried out in TiO<sub>2</sub>, Ag-TiO<sub>2</sub>, and rutile in the same photo-reaction condition. Compared with the pure TiO<sub>2</sub> and rutile, the Ag-TiO<sub>2</sub> shows an obvious enhancement in the MR photo degradation under UV light irradiation, which could be attributed to the Ag nanoparticles by acting as electron traps.

### Acknowledgments

The authors are thankful to Dr. Mamata Tripathy Department of Zoology Assistant Professor University of Delhi. My inspired faculty.

### References

1. Díaz-Urbe, Carlos, *et al.* Photocatalytic activity of Ag-TiO<sub>2</sub> composites deposited by photoreduction under

UV irradiation. International Journal of Photoenergy; c2018.

2. Elsalamony RA. Advances in photo-catalytic materials for environmental applications. Res Rev J Mat Sci. 2016;4(2):26-50.
3. Elsalamony RA. Advances in photo-catalytic materials for environmental applications. Res Rev J Mat Sci. 2016;4(2):26-50.
4. Mathew EY, Dodo JD, Maton SM, Dalen MB. Assessment of persistent organic pollutants in soil and water of Kara Bisichi, Barkin Ladi Lga of Plateau state, Nigeria. Int. J Adv. Chem. Res. 2021;3(2):04-11. DOI: 10.33545/26646781.2021.v3.i2a.35
5. Cao G. Nanostructures & Nanomaterials: Synthesis, Properties & applications, Imperial College Press, London, UK; c2004.
6. Gowthambabu V, *et al.* ZnO nanoparticles as efficient sunlight driven photocatalyst prepared by solution combustion method involved lime juice as biofuel. Spectrochimica Acta Part A: Molecular and Biomolecular Spectroscopy. 2021;258:119857.
7. Mahshid Sara, Askari M, Sasani Ghamsari M. Synthesis of TiO<sub>2</sub> nanoparticles by hydrolysis and peptization of titanium isopropoxide solution. Journal of materials processing technology. 2007;189(1-3):296-300.
8. Mehr, Masoud Emami, *et al.* Synthesis and characterization of photocatalytic zinc oxide/titanium oxide (core/shell) nanocomposites. Journal of Alloys and Compounds. 2021;882:160777.
9. Nateq Mohammad Hossein, Riccardo Ceccato. Sol-gel synthesis of TiO<sub>2</sub> nanocrystalline particles with enhanced surface area through the reverse micelle approach. Advances in Materials Science and Engineering; c2019.
10. Sasikala R, *et al.* Role of support on the photocatalytic activity of titanium oxide. Applied Catalysis A: General. 2010;390(1-2):245-252.
11. Sasikala R, Shirole AR, Sudarsan V, Kamble VS, Sudakar C, Naik R, *et al.* Role of support on the photocatalytic activity of titanium oxide. Applied Catalysis A: General. 2010 Dec 20;390(1-2):245-52
12. Zhou Rui, *et al.* Continuous synthesis of Ag/TiO<sub>2</sub> nanoparticles with enhanced photocatalytic activity by pulsed laser ablation. Journal of Nanomaterials; c2017.
13. Eric DK. Nano system Molecular machinery, Manufacturing and computation, Doubleday; c1992.